Expert Systems With Applications 243 (2024) 122934

Contents lists available at ScienceDirect

Expert Systems With Applications

journal homepage: www.elsevier.com/locate/eswa

Identifying HRV patterns in ECG signals as early markers of dementia

Juan E. Arco [a,b,c,*], Nicolás J. Gallego-Molina [b], Andrés Ortiz [b,c], Katy Arroyo-Alvis [d], P. Javier López-Pérez [e]

[a] Department of Signal Theory, Networking and Communications, University of Granada, 18010 Granada, Spain
[b] Department of Communications Engineering, University of Malaga, 29010 Malaga, Spain
[c] Data Science and Computational Intelligence Institute (DaSCII), University of Granada, Spain
[d] Corporación Universitaria del Caribe-CECAR, Colombia
[e] Department of Social Sciences, Universidad de la Costa, Colombia

ARTICLE INFO

Keywords:
Heart rate variability
Mild cognitive impairment
Dementia
Machine learning
Signal processing

ABSTRACT

The appearance of Artificial Intelligence (IA) has improved our ability to process large amount of data. These tools are particularly interesting in medical contexts, in order to evaluate the variables from patients' screening analysis and disentangle the information that they contain. We propose in this work a novel method for evaluating the role of electrocardiogram (ECG) signals in the human cognitive decline. This framework offers a complete solution for all the steps in the classification pipeline, from the preprocessing of the raw signals to the final classification stage. Numerous metrics are computed from the original data in terms of different domains (time, frequency, etc.), and dimensionality is reduced through a Principal Component Analysis (PCA). The resulting characteristics are used as inputs of different classifiers (linear/non-linear Support Vector Machines, Random Forest, etc.) to determine the amount of information that they contain. Our system yielded an area under the Receiver Operating Characteristic (ROC) curve of 0.80 identifying Mild Cognitive Impairment (MCI) patients, showing that ECG contain crucial information for predicting the appearance of this pathology. These results are specially relevant given the fact that ECG acquisition is much more affordable and less invasive than brain imaging used in most of these intelligent systems, allowing our method to be used in environments of any socioeconomic range.

1. Introduction

We are living currently in a world with a high amount of data. Unlike other previous periods in history, the problem now is that there are much more data than means of processing it. In fact, having data itself is not beneficial if we cannot process them, which implies that it is crucial to separate information from noise. This is particularly interesting in medicine, where routine analysis provide us a number of variables that summarize the health of the patient. Most important, these descriptors can be potentially used to predict the future outcome of the patient's health based on the present information. The application of Artificial Intelligence (AI) to the analysis of this data has revolutionized the identification of several pathologies. In fact, previous studies have proposed models for an early detection of neurological disorders such as Alzheimer's (Arco, Ortiz, Castillo-Barnes, Górriz, & Ramírez, 2023; Arco, Ortiz, Gallego-Molina, Górriz, & Ramírez, 2023; Arco, Ramírez, Górriz, & Ruz, 2021; Wang et al., 2023; Arco et al., 2019) or Parkinson's (Arco, Ortiz, Castillo-Barnes, Górriz, & Ramírez, 2022; Arco, Ortiz, Ramírez, et al., 2023; Coelho et al., 2023; Sigcha et al., 2023), and for a distinction between different pulmonary affections (Alizadehsani et al., 2021; Arco, Ortiz, Ramírez, et al., 2022). Although these works rely on medical imaging, it is possible to analyze other physiological signals to determine the diagnosis of a patient, such as electroencephalography (EEG) signals, which are extraordinarily relevant for the study of dyslexia (Gallego-Molina, Ortiz, Martínez-Murcia, Formoso, & Giménez, 2022; Rodríguez-Rodríguez, Ortiz, Gallego-Molina, Formoso, & Woo, 2023; Štajner, Saggion, & Ponzetto, 2019; Wang & Bi, 2022) or epilepsy (Abou-Abbas, Henni, Jemal, Mitiche, & Mezghani, 2023; Beniczky, Karoly, Nurse, Ryvlin, & Cook, 2021; Bosl, Leviton, & Loddenkemper, 2021; Ilias, Askounis, & Psarras, 2023).

Heart rate variability (HRV) refers to the fluctuation in the time interval between successive heartbeats or the variation in the heart rate itself. This metric has been increasingly adopted in both clinical and research applications (Billman, 2015). Notably, a comprehensive

* Corresponding author at: Department of Signal Theory, Networking and Communications, University of Granada, 18010 Granada, Spain.
E-mail addresses: jearco@ugr.es (J.E. Arco), njgm@ic.uma.es (N.J. Gallego-Molina), aortiz@ic.uma.es (A. Ortiz), katy.arroyoa@cecar.edu.co (K. Arroyo-Alvis), plopez10@cuc.edu.co (P.J. López-Pérez).

https://doi.org/10.1016/j.eswa.2023.122934
Received 19 June 2023; Received in revised form 9 December 2023; Accepted 10 December 2023
Available online 15 December 2023

review explored the connection between HRV in wellness and illness, highlighting that variations in HRV can provide insight into the operations of the sympathetic and parasympathetic systems (Kristal-Boneh, Raifel, Froom, & Ribak, 1995). Another piece of research proved the correlation between HRV and coronary artery disease, uncovering that HRV exhibits irregularities in several instances of ischemic heart disease (Huikuri, 1995). Additionally, a separate study explored the link between HRV and inflammation indicators in cardiovascular diseases, concluding that HRV has a relation with circulating cytokines in cardiovascular functionality in humans (Haensel, Mills, Nelesen, Ziegler, & Dimsdale, 2008). Other studies have focused on how HRV affects critical illness and care (Buchman, Stein, & Goldstein, 2002), as well as lupus disease activity (Thanou et al., 2016), and kidney failure (Ranpuria, Hall, Chan, & Unruh, 2007).

HRV is often viewed as a reflection of the well-being of the autonomic nervous system (ANS), which is crucial for controlling essential body operations such as heart rate, blood pressure, digestion, and respiration. Additionally, the ANS plays a role in modulating cerebral blood circulation, which is key for supplying the brain with oxygen and nutrients. Increasingly, research indicates that compromised ANS performance could potentially lead to cognitive deterioration and dementia. Past research has highlighted a link between diminished HRV and a heightened risk of cognitive impairment and dementia (Forjanski et al., 2019), including Alzheimer's disease (O'Brien, Hinder, Callaghan, & Feldman, 2017). This association may be explained by several possible mechanisms. For example, a reduced HRV may reflect impaired ANS function, which may in turn affect cerebral blood flow and contribute to the development of cognitive decline (Boissoneault, Letzen, Robinson, & Staud, 2019). Other potential explanations for the relationship between HRV and dementia include the effects of cardiovascular risk factors such as hypertension and diabetes (Liao et al., 1995). In addition, chronic inflammation could also play a crucial role, as inflammation is known to affect both ANS function and cognitive function (Weinstein, Davis-Plourde, Beiser, & Seshadri, 2021).

Based on these studies, scientists are currently investigating the potential role of HRV as a predictive or diagnostic marker for dementia, as a sign of early cognitive decline, or even to pinpoint individuals who are at an elevated risk of developing this disorder (Chou et al., 2022; Wang et al., 2019). Numerous studies have focused on investigating the relationship between HRV and cognitive capabilities across various populations, ranging from baseline condition to cognitive impairment-induced decline. Forte, Favieri, and Casagrande (2019) presented a thorough examination of these two indicators, suggesting HRV could potentially be recognized as an early biomarker of cognitive impairment. Yet another study demonstrated that HRV is positively correlated with cognitive functions in older men (Yang et al., 2008). Conversely, different studies have examined the autonomic behavior in the context of Alzheimer's disease (AD) and vascular dementia (VAD), indicating that no substantial disparity exists in HRV parameters between these two dementia categories and the control group (Allan et al., 2005). Nevertheless, a more contemporary research observed an association between diminished HRV and deteriorated cognitive capabilities in multiple areas like attention, executive function, and memory, in a population with no signs of dementia (Schaich et al., 2020).

In this work, we propose a novel approach for evaluating the informativeness of electrocardiogram (ECG) signals and their influence in the human cognitive decline. Our method proposes a complete framework for the study of this kind of signals that covers the entire pipeline: from the preprocessing of the HRV measures to the application of Principal Component Analysis (PCA) for feature extraction. The information retrieved by these embeddings are then entered into a Support Vector Machines (SVM) classifier. Then, we evaluated the performance of this proposal in ECG signals from controls and patients who suffered from Mild Cognitive Impairment (MCI), aimed at exploring if the joint of AI and HRV can be used as an early marker of the risk of developing dementia.

The methodology presented skillfully employs machine learning within a classification framework where differences between HRV in different groups of patients are evaluated. The work is organized as follows: Section 2 provides a summary of previous studies on HRV and ECG signal analysis. Section 3 includes a comprehensive description of the database, in addition to explain the various methods proposed in this study, including the preprocessing pipeline and feature extraction prior to the classification stage. In Section 4, the method's ability to detect differences in physiological signals and cognitive states is evaluated. Besides, this section details the experiments conducted. Results are outlined in Section 5, followed by a discussion of their implications in Section 6. Section 7 finally provides a summarization of the research along with potential paths for future investigations.

2. Related works

The study of the factors that affect human cognitive decline is crucial for an early diagnosis of disorders such as AD. In fact, the identification of variables with a high correlation with cognitive deficits has been one of the research lines followed by recent studies. Many of them have successfully revealed important aspects that had not been previously considered. For example, Chen et al. (2023) found that a reduced slow-wave activity and autonomic dysfunction during sleep precede cognitive deficits related to AD. Specifically, they mentioned that sleep problems and autonomic dysregulation could play a crucial role at the early stages of the disease. It seems clear that there are uncountable factors that can affect human health, and thus the complexity for an early diagnosis is maximum. The inclusion of AI-based systems try to mitigate this difficulty by developing automatic systems that help in the diagnostic process (Calisto et al., 2023; Sun, Zhang, Wang, & Tiwari, 2023). For example, AI tools have demonstrated an excellent performance when focusing on the pharmacology and molecular docking prediction related to cognitive dysfunction (Han et al., 2023). However, the most classical perspective is to employ these systems in the processing and analysis of medical images (Calisto, Nunes, & Nascimento, 2020). There is a wide range of image modalities to which these algorithms are applied to, such as ultrasound (Feng et al., 2023), computerized tomography (CT) (Arco et al., 2022b), or magnetic resonance (MR) (Górriz et al., 2023) images. Given the complementary information that different modalities provide, some studies have proposed solutions for the registration of multi-modal images based on a disentangled convolutional sparse coding model (Deng, Liu, Li, Duan, & Xu, 2023). One of the most important research lines is related to human–computer interaction (HCI), highlighting how technology can assist individuals with functionality declines (Bhardwaj, Jutai, & Fallavollita, 2023). AI models need to be accurate but also provide explanations about the human behavior that allow the continuous improvement of these systems. Following a similar pipeline, Lv, Yu, Xie, and Alamri (2022) modified a convolutional neural network (CNN) as the basis of a platform that evaluates the healthcare based on a high number of variables. The idea is not only to improve the diagnostic and treatment process, but to improve the efficiency in different medical contexts such as surgical procedures or the treatment patients' privacy information.

The high applicability of AI models has also been shown in the assessment of electrocardiogram (ECG) signals and HRV for detecting and preventing various heart conditions. This is especially relevant in a context where the analysis and interpretation of signals is extremely complex, and conventional processing techniques have limitations in the detection of different pathologies. Intelligent systems based on machine (ML) and deep learning (DL) techniques have identified different cardiac conditions such as arrhythmia or myocardial infarction (MI) (Murat et al., 2021; Nezamabadi, Sardaripour, Haghi, & Forouzanfar, 2023). Li, Yuan, Wang, Cui, and Cao (2016) proposed an architecture for the automatic detection of arrhythmia based on multimodal features. Specifically, they employed a Kernel-Independent Component

Analysis (KICA) to address the complexity in feature extraction of nonlinear scenarios (Bach & Jordan, 2003), and a discrete wavelet transform (Alessio, 2006) for analyzing the information contained in ECG beats. Then, the resulting features were entered into a classifier through an optimization with a genetic algorithm. The proposed system led to an accuracy of 97.3% for the identification of cardiac arrhythmias. Other studies have focused on MI detection and ischemia based on T-wave abnormalities and ST-segment. Hadjem, Naït-Abdesselam, and Khokhar (2016) employed random user sampling (RUS) techniques for solving the class imbalance problem present in most of ECG studies, in combination with a hybrid boosting algorithm for oversampling (Seiffert, Khoshgoftaar, Hulse, & Napolitano, 2010). The classifier relied on an ensemble of weak classifiers based on decision trees, achieving a good performance in datasets with different balances between classes. The problem of many ST-segment monitoring systems is the high amount of excessive false positive alarms that they provide, even when using strict trigger thresholds. Based on the ECG tracings employed by cardiologists, Xiao et al. (2018) presented an image-based alternative based on DL through a transfer-learning scheme. The idea behind this study was the conversion of the ST changes into a computer vision task, in order to take advantage of the tools available for image processing in the context of ECG signals. Specifically, they employed a pretrained model based on the Inception one (Szegedy et al., 2015) to identify the images with significant ST changes. Results showed a precise detection of these changes even when they had a short duration, offering valuable information about the temporal patterns associated with cardiac disorders.

It is also important to mention the role that HRV has not only in cardiac episodes, but also in other pathologies that are not supposed to be related to heart failure. Previous studies have demonstrated that intelligent systems can extract vital information from the HRV in the different phases of epileptic seizures (Yamakawa, Miyajima, Fujiwara, Kano, Suzuki, Watanabe, Watanabe, Hoshida, Inaji, & Maehara, 2020a). These systems are based on the idea that seizures are preceded by modifications in the heart rate, as previously demonstrated in Lotufo, Valiengo, Benseñor, and Brunoni (2012). An optimum extraction of the information contained in HRV is crucial for the development of a robust architecture that allows the identification of a specific anomaly. Previous works have focused on defining variables from HRV signal, such as the RR intervals (i.e. the time between successive heartbeats), which seem extremely informative as shown by Yamakawa, Miyajima, Fujiwara, Kano, Suzuki, Watanabe, Watanabe, Hoshida, Inaji, and Maehara (2020b). Specifically, they extracted information from HRV signals by using a Multivariate Statistical Process Control (MSPC) method (Morris & Samad, 2021), in terms of two statistics. According to the value of these two variables, a discriminative threshold was empirically set in order to determine the appearance (or not) of the seizure. Results obtained by Chen, Liu, Su, Jiang, and Nguyen (2017) showed again the informativeness of RR intervals, designing an autoencoder for congestive heart failure (CHF) detection, leading to a robust solution with a high performance.

3. Methodology

3.1. Participants

A cross-sectional study of an exploratory nature was carried out with 36 participants originating from Sincelejo, Colombia. The cohort was split into two categories: Controls (CTL) and individuals with Mild Cognitive Impairment (MCI). The latter group included 18 individuals diagnosed with amnestic MCI (average age = 70.2, 12 of them males and 6 females, mean education level = 12.3 years, and an average Mini Mental State = 23.8), as directed by local memory health clinics. The control group was comprised of 18 participants bearing similar socio-demographic characteristics (average age = 67.9, 14 of whom were males and 4 females, mean education level = 12.2 years, and Mini Mental State = 28.7). The design of the study incorporated exclusion criteria grounded on medical conditions and medications that have been proven to significantly affect HRV (Nicolini et al., 2014, 2022). These included: (a) departure from regular sinus rhythm, such as atrial fibrillation, alternate arrhythmias, and paced rhythms, (b) cardiovascular anomalies like coronary artery disease and heart failure, along with diabetes mellitus, neurological and psychiatric conditions (including Parkinson's disease, stroke, and acute depression) and other serious diseases (respiratory, renal, autoimmune, and neoplastic), (c) medicines affecting cardiac function: beta-blockers, alpha-blockers, centrally-acting calcium-channel blockers, class I and III antiarrhythmic medicines, and digoxin, (d) psychotropic medications: tricyclic antidepressants, selective serotonin-noradrenaline reuptake inhibitors, non-traditional antidepressants, antipsychotics, and cholinesterase inhibitors. Diagnostic procedures were performed by certified neuropsychologists and neurologists associated with memory health clinics. For the purpose of this investigation, an independent examination was carried out, the details of which are outlined in the subsequent section.

3.2. Neuropsychological test battery

The neuropsychological evaluation was carried out following the evaluation protocol composed of standardized tests in the Colombian population including different cognitive domains. They include episodic memory, executive functioning, visuospatial skills, praxis and language. A summary of the neuropsychological tests used is presented below:

- Benton Visual Retention Test: evaluates visuoconstruction skills, associative, spatial and visual perception, as well as components of immediate visual memory and selective attention (Benton, 1974).
- Benton Visual Shape Discrimination Test: determines skills related to visual perception and discrimination through visual matching and abstract memory processes (Benton, 1983).
- Boston Vocabulary Naming Test: examines naming ability from the verbal-visual component, where through images its illustration, naming and meaning are detailed, using an adaptation to Latin American countries of the Spanish version (Duarte Pedroza, Espitia, & Montañés, 2016).
- Striated Pegboard test: measures motor speed, manual skills, fine motor control and oculo-motor coordination (Trites, 2023).
- Wisconsin Card Sorting Test (128 cards): assesses cognitive factors of executive functioning, especially functions of planning, organization and reasoning, mediated thinking, adaptation to change and abstraction (Grant & Berg, 1948).
- Rey Auditory Verbal Learning Test: determines the functionality of memory, especially auditory memory, examining encoding, storage and recall of information, also measuring selective and sustained attentional processes (Rey, 1941).
- Trail Making Test A and B (TMT A and B): examines cognitive executive functions, detailing attentional performance, perception, abstraction through visuo-motor sequencing and working memory and especially processing speed, working memory, abstraction, sequencing, monitoring (Bowie & Harvey, 2006).
- Controlled word association test (FAS): determines verbal fluency performance, based on phonological identification, use of mental configuration, working memory, self-monitoring and executive search (Lezak et al., 2004).
- Stroop's color and word test: assesses alternating-type attentional skills, cognitive functions, inhibitory capacity and interference control (Stroop, 1935).
- Rey-Osterrieth (RO) complex figure test (copying and evocation): examines cognitive abilities such as planning and organization of information, through visuoconstructional, perceptual, spatial and practical skills, as well as immediate visual memory (Rey, 2009).

Table 1
Differences in the results of the neuropsychological tests between MCI and CTL groups. The comparison between groups in terms of most of the tests lead to extremely low *p*-values, highlighting the significant differences between groups.

Variable	CTL	MCI	*p-value*
MMSE	28.7 ± 1	23.8 ± 3	0.001
Boston correct without key	61 ± 4.9	40.2 ± 9.1	0.001
Pins right hands time	76.9 ± 18.2	143.1 ± 64.4	0.001
Wisconsin hits	68.2 ± 11.4	32.6 ± 21.5	0.001
Wisconsin errors	48.2 ± 19.7	56.5 ± 14	0.15
Wisconsin categories	4.2 ± 1.9	1 ± 1.4	0.001
Wisconsin perseverative responses	23.8 ± 12.9	15.4 ± 24.5	0.2
Pins right hands time	76.9 ± 18.2	143.1 ± 64.4	0.001
Wisconsin initial conceptualization	22.4 ± 18.9	10.5 ± 17	0.05
Wisconsin conceptual level response	55.6 ± 16	21.3 ± 22.6	0.001
Wisconsin failures to maintain principle	1.2 ± 1.2	0.7 ± 1.1	0.22
Auditory-verbal learning a1	4.4 ± 0.9	2.9 ± 1	0.001
Auditory-verbal learning a5	8.8 ± 2.2	6.5 ± 2.6	0.006
Auditory-verbal learning b	3.6 ± 1.6	1.8 ± 1.3	0.001
Auditory-verbal learning a6	7.8 ± 2.3	4.6 ± 2.2	0.001
Auditory-verbal learning a7	7.4 ± 2.4	3.1 ± 2.6	0.001
Visual discrimination Benton	29.4 ± 3.4	21.5 ± 5	0.001
TMT A time	53.9 ± 22.6	134.6 ± 109.1	0.004
TMT A errors	0 ± 0	3.3 ± 5.4	0.012
TMT B time	109.8 ± 41.1	217.9 ± 145.7	0.004
TMT B errors	1.8 ± 3.7	11.7 ± 8.7	0.001
Total phonological fluency	33.6 ± 9.7	20.2 ± 10.8	0.001
Stroop reading	81.4 ± 13.2	42.6 ± 20.8	0.001
Stroop color	61.4 ± 14.9	35.3 ± 14.4	0.001
Stroop conflict	49.8 ± 19.3	18.9 ± 9.6	0.001
RO complex figure total copy	32.1 ± 3.9	23.8 ± 7.8	0.001
RO complex figure copying time	194.1 ± 100.3	362.7 ± 193.5	0.002
RO complex figure total memory	15.6 ± 5.4	5.3 ± 4.2	0.001
RO complex figure memory + time	139.2 ± 64.6	163.3 ± 80.6	0.32
Katz	0 ± 0	0.3 ± 0.8	0.1
Lawton	8.2 ± 0.5	12.9 ± 4.6	0.001
Barthel	50 ± 0	49.4 ± 1.6	0.15
Yesavage	1.8 ± 2.4	2.1 ± 1.7	0.69

- Folstein Mini-Mental State Examination (MEEM): examines various aspects of global cognitive performance, determining the functioning of several cognitive areas such as orientation, calculation, immediate recall, language, reading, writing, praxis and visuospatial function (Barrero, Vives, & Morales, 2006; Folstein, Folstein, & McHugh, 1975).

The results from the neuropsychological tests were analyzed using one-way analysis of variance, whereas for continuous variables an ANOVA or the Kruskal–Wallis test was used. Table 1 summarize the results of the different tests for both groups (CTL and MCI), as well as their statistical significance. It is clear the high differences found between the two groups, which demonstrate how different they are from a cognitive perspective. In fact, differences in terms of most of the tests of the battery are extremely significative, leading to *p*-values much lower than 0.05.

3.3. ECG acquisition

The main idea of this work is to find the previously mentioned differences between control and MCI groups in ECG signals. The process of data acquisition adhered to the Declaration of Helsinki and respected bioethical norms. Before each HRV recording, informed consent was obtained in accordance with the protocol approved by the Ethics Committee of the University of la Costa, Colombia (Code 072). The equipment utilized for data capture was the BWII EEG, accompanied by the Neurovirtual BWII Analysis software (https://neurovirtual.com/). For each one of the 36 participants described in Section 3.1, the EEG recordings followed the 10-20 system, and maintained a sampling frequency of 200 Hz. They were also subjected to a 50/60 Hz filter, in addition to a digital filter, both as per the guidelines provided by the manufacturer's software.

3.4. Preprocessing

Once the ECG signals were acquired, we focused on the analysis of HRV, which is a popular biomarker that can offer interesting information about the patient's health. Heart rate refers to the quantity of heartbeats occurring within a minute, while HRV quantifies the duration of the interval between successive heartbeats. Mccraty and Shaffer (2015). Fig. 1 shows a representation of the first 2000 samples of an ECG signal. The first step to quantify the HRV relies on the computation of the distances between consecutive peaks in the ECG waveform. When peaks that show abnormal measures are discarded and calculations only focused on normal peaks, these distances are known as Normal-to-Normal Intervals (NNI), as follows:

$$NNI_j = R_{j+1} - R_j \quad \text{for} \quad 0 \le j \le n-1 \tag{1}$$

where NNI_j represents the value of the NNI at sample j, R_j and R_{j+1} refer to two consecutive peaks and n is the number of peaks.

One important aspect in the preprocessing of this kind of signals is to eliminate the different artifacts that they usually contain. In fact, the presence of any artifact within the NNI can potentially disrupt the analysis of these signals. These artifacts may be originated from either technical factors, such as noise or imprecise detection algorithms, or physiological factors, including arrhythmic events and ectopic beats (Lippman, Stein, & Lerman, 1993, 1994; Tarvainen, Niskanen, & Lipponen, 2014). Manually checking for artifacts is considered the best practice in a clinical setting. However, this process can be time-consuming, particularly for long-term recordings, and may become especially tedious. We employed an automatic algorithm based on the differences between successive NNI. First, an estimated threshold is derived from the time-varying distribution of the NNI series. Initially, a threshold was determined by analyzing the time-varying distribution of the NNI series. For each beat, the quartile deviation of the 90 surrounding beats was computed and then multiplied by a factor of

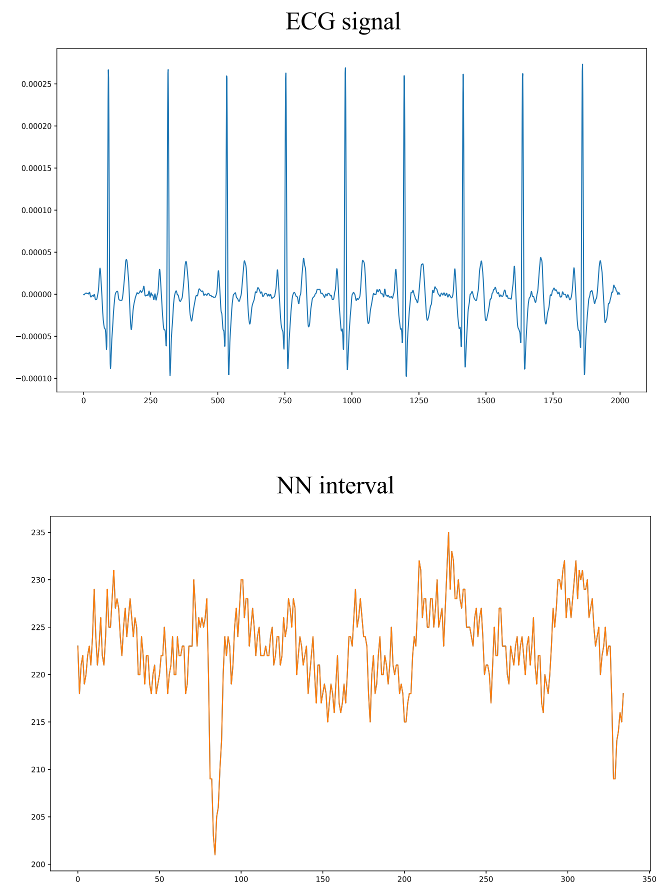

Fig. 1. Representation of an ECG signal (top) and an NN interval (bottom).

Table 2
Time-domain measures of the HRV.

Time-domain features	
Mean NNI	Average duration of the NNI
Median NNI	Median duration of the NNI
Range NNI	Range duration of the NNI
SDNN	Standard deviation of all NNIs
CVNNI	Ratio between the SDNN and the mean NNI
SDSD	Standard deviation of the differences between successive NNIs
NNI50	Number of NNIs greater than 50 ms
PNNI50	Ratio between NNI50 and the total number of NNIs
NNI20	Number of NNIs greater than 20ms
PNNI20	Ratio between NNI20 and the total number of NNIs
RMSSD	Root mean square of the sum of successive differences
CVSD	Coefficient of variation between successive NNIs
Mean HR	Average heart rate
Max HR	Maximum heart rate
Min HR	Minimum heart rate
SD HR	Standard deviation of the heart rate
TI	Triangular Index
TINN	Triangular interpolation of the NNI Histogram

5.2. This amplified range encompassed 99.95% of all beats, assuming a normal distribution of the NNI series. This approach ensures accurate detection across a wide range of scenarios. Subsequently, any values identified as outliers or ectopic beats were eliminated from the signal.

Once the signal is cleaned, the next step is to compute different features that summarize the information contained in the NNI (Task Force of The European Society of Cardiology and The North American Society of Pacing and Electrophysiology, 1996). In order to maximize the robustness of the method, we computed features based on measures from different sources that can be summarized according to their origin:

Table 3
Frequency-domain measures of the HRV.

Frequency-domain features	
VLF	Power of very low-frequency bands
LF	Power of low-frequency bands
HF	Power of high-frequency bands
Total power	Power in the band from very low-frequency to high-frequency.
LF-HF ratio	Ratio between the power of LF and HF bands
LF-nu	Ratio between the power of LF and the power in LF and HF bands
HF-nu	Ratio between the power of HF and the power in LF and HF bands

time domain, frequency domain and non-linear measurements (Shaffer & Ginsberg, 2017).

3.4.1. Temporal domain

HRV time-domain indicators quantify the variability in measurements linked to the intervals between successive heart beats. As such, most of these indicators originate from the NNI. Basic metrics can be calculated by determining the average of the NNI, its standard deviation (SDNN), or the deviation in the differences between consecutive NNIs. Additional features arise from the count of NNIs exceeding a certain duration (e.g., 20 or 50 ms) and the ratio of NNIs surpassing these durations to the total count. Other common metrics related to heart rate include maximum or minimum values or statistics based on average or standard deviation. Furthermore, two variables based on data geometry were incorporated: the Triangular Index (TI) and the Triangular Interpolation of the NNI histogram (TINN). The former is calculated as the density distribution's integral divided by its maximum, while the latter represents the baseline width of the distribution, measured as a triangle base (Hämmerle et al., 2020), offering an estimate of the NNI distribution (Rubin, Abreu, Ahern, Eldardiry, & Bobrow, 2016). A summary of all utilized time-domain features can be found in Table 2.

3.4.2. Frequency domain

HRV frequency-domain metrics offer insights into how variance is allocated across the frequency spectrum. Often referred to as power spectral density analysis (Cha et al., 2018), these metrics have been applied in the past to discern irregularities in sympathetic and parasympathetic systems (Hillebrand et al., 2013). The objective of these measurements is to estimate power distributions across various frequency bands: Very-Low-Frequency (VLF, $0.0033 < f < 0.04$ Hz), Low-Frequency (LF, $0.05 < f < 0.15$ Hz), and High-Frequency (HF, $0.15 < f < 0.40$ Hz). Hence, the most basic measures stem from the power of the HRV in these three bands, in either absolute or relative terms. More specifically, normalized spectral indices are defined as the percentage of power in a particular band from the total power of the entire spectrum, as follows:

$$LF_{nu} = \frac{LF}{LF + HF} \tag{2}$$

$$HF_{nu} = \frac{HF}{LF + HF} \tag{3}$$

Table 3 summarizes the different frequency-domain features employed in this work.

3.4.3. Non-linear measurements

The variables captured by HRV may exhibit non-linear characteristics, implying that their relationship cannot be represented by a simple straight line on a plot. One of the primary benefits of non-linear measures is their insensitivity to changes in trends of the NNI (Behbahani, Jafarnia Dabanloo, & Motie Nasrabadi, 2013). The most common non-linear variables are derived from the Poincaré plot (Hoshi, Pastre, Vanderlei, & Godoy, 2013), which is obtained by plotting every NNI against the prior interval. When the plot is conformed to match an ellipse, three variables can be derived: $SD1$, $SD2$, and their ratio

Table 4
Non-linear measures of the HRV.

Non-linear measurements	
SD1	Standard deviation of Poincaré plot perpendicular to the line-of-identity
SD2	Standard deviation of the Poincaré plot along to the line-of-identity
CSI	Cardiac sympathetic index
CVI	Cardiac vagal index
Modified CSI	Modified cardiac sympathetic index
SampEn	Sample Entropy

($SD1/SD2$). The former two align with the breadth and length of the ellipse, symbolizing the standard deviation of instantaneous variability between successive beats and consistent NNI long-term variability, correspondingly (Bhaskar & Ghatak, 2013). These variables are critical as they share correlations with other significant measurements. For instance, $SD1$ quantifies short-term HRV and aligns with baroreflex sensitivity, which is instrumental in evaluating neural control of cardiovascular function (Rovere, Maestri, & Pinna, 2011). Conversely, $SD2$ is associated with both short- and long-term HRV, as well as BRS and power in low frequencies (Brennan, Palaniswami, & Kamen, 2001). Lastly, the ratio $SD1/SD2$ serves as a metric for the unpredictability of the NNI and is perceived as an indication of autonomic equilibrium during sympathetic activation (Shaffer & Ginsberg, 2017).

It is important to note that the ratio $SD1/SD2$ is also known as Cardiac Sympathetic Index (CSI). Moreover, slight modifications in the relationship between $SD1$ and $SD2$ lead to two different measures widely used in the cardiac conditions: the modified Cardiac Sympathetic Index (MCSI) and the Cardiac Vagal Index (CVI), which can be computed as follows:

$$MCSI = \frac{SD1^2}{SD2} \qquad CVI = \log_{10}(SD1 \cdot SD2) \tag{4}$$

The last non-linear parameter computed was the Sample Entropy (SampEn), which represents the conditional probability that two vectors, that are closely positioned in m dimensions, will continue to remain close in the subsequent $m+1$. Thus, this variable quantifies the regularity and the complexity of the time series evaluated. All the non-linear measurements employed in this work are summarized in Table 4.

For the computation of all these features, we utilized custom code and the pyHRV software (Gomes, Margaritoff, & Silva, 2019). Fig. 2 illustrates how CTL and MCI patients differ according to some of the features computed, such as the distribution of the NNI histogram, the Power Spectral Density (PSD) and the average NNI duration and TIN.

3.5. Feature extraction

The classification of high-dimensional data possessing a small sample size brings forth a notorious challenge (Raudys & Jain, 1991). Datasets usually have more features than samples, making the problem more severe. Hence, a viable solution to circumvent this problem is necessary. A method that has received extensive recognition for this purpose is Principal Component Analysis (PCA) (Jolliffe, 1986; Khedher, Ramírez, Górriz, Brahim, & Segovia, 2015; López, Ramírez, Górriz, Salas-Gonzalez, et al., 2009). For a given set of N samples $\mathbf{x}_k$, $\mathbf{x}_k = [\mathbf{x}_{k1}, \dots, \mathbf{x}_{kn}] \in \mathbb{R}^n$, PCA aims to reduce the data's dimensionality by identifying a lower-dimensional linear subspace that retains the maximum data variance (López, Ramírez, Górriz, Illan, et al., 2009). However, there are instances where feature extraction via linear methods is not viable. In these cases, Kernel PCA (Schölkopf, Smola, & Müller, 1998; Wang, 2012) projects the input vector $\mathbf{x}$ from the $\mathbb{R}^n$ space to a high-dimensional feature space $\mathbb{R}^f$ using a non-linear mapping function $\boldsymbol{\Phi} : \mathbb{R}^n \rightarrow \mathbb{R}^f, f > n$. The eigenvalue problem in the new feature space, $\mathbb{R}^f$, can be formulated as shown:

$$C^{\Phi}\mathbf{w}^{\Phi} = \lambda \mathbf{w}^{\Phi} \tag{5}$$

where C^{Φ} symbolizes the covariance matrix. The solution set $\mathbf{w}^{\Phi}$ for $\lambda \neq 0$ can be found in the transformed space $\Phi(\mathbf{x}_1, \dots, \Phi(\mathbf{x}_N))$. Furthermore, there exist coefficients α_i that uphold the relationship:

$$\mathbf{w}^{\Phi} = \sum_{i=1}^{N} \alpha_i \Phi(\mathbf{x}_i) \tag{6}$$

An $N \times N$ matrix K is defined by

$$K_{ij} = k(\mathbf{x}_i, \mathbf{x}_j) = \Phi(\mathbf{x}_i) \cdot \Phi(\mathbf{x}_j) \tag{7}$$

as a result of which the PCA problem is reformulated:

$$N\lambda K\boldsymbol{\alpha} = K^2\boldsymbol{\alpha} \equiv N\lambda\boldsymbol{\alpha} = K\boldsymbol{\alpha} \tag{8}$$

where $\boldsymbol{\alpha}$ is a column vector with entries $\alpha_1, \dots, \alpha_N$ (Schölkopf et al., 1998).

A variant of PCA, employing a nonlinear kernel, can introduce a nonlinear form to PCA. One of these kernels is the radial basis function (RBF), which can be expressed as:

$$k(\mathbf{x}i, \mathbf{x}j) = exp\left(-\frac{1}{2}\frac{\|\mathbf{x}i - \mathbf{x}j\|^2}{\sigma^2}\right) \tag{9}$$

Upon mapping the dataset to a space of higher dimensions, the vectors are subsequently projected onto a subspace of lower dimensions, defined by the eigenvectors $\mathbf{w}^{\Phi}$. Given a sample $\mathbf{x}$ and its corresponding projection $\Phi(\mathbf{x})$ within the higher-dimensional space $\mathbb{R}^f$, the projection of $\Phi(\mathbf{x})$ onto the eigenvectors $\mathbf{w}^{\Phi}$ constitutes the nonlinear principal components in accordance with the mapping function Φ. This can be mathematically represented as:

$$\mathbf{w}^{\phi} \cdot \Phi(\mathbf{x}) = \sum_{i=1}^{N} \alpha_i (\Phi(\mathbf{x}_i)\Phi(\mathbf{x})) = \sum_{i=1}^{N} \alpha_i K(\mathbf{x}_i, \mathbf{x}) \tag{10}$$

This newly formulated subspace is spanned by the dominant eigenvectors associated with the covariance matrix, as characterized in Eq. (5). To preserve a satisfactory quantum of variance, only the bare minimum number of eigenvectors accounting for 90% of the overall variance are earmarked for the classification phase.

3.6. Classification

The resulting components were subsequently employed as the input variables for the classification algorithm. Specifically, we used the Support Vector Machines (SVM) classifier, which is structured around a decision function aimed at maximizing the geometric margin between the two categories. The classification rule, denoted by f, is determined from two input vectors $(\mathbf{x}, \mathbf{x_i})$, as depicted below:

$$f(\mathbf{x}_i) = \langle \mathbf{w}, \mathbf{x}_i \rangle + b \tag{11}$$

Here, $\mathbf{w}$, $\mathbf{x}_i$ and b represent the weights, the feature vector, and the error term correspondingly. The sample x is categorized as positive or negative depending on whether $f(x)$ exceeds or is less than 0. Hence, the decision function depends around a rule generated via the solution of the optimization problem detailed in Boser, Guyon, and Vapnik (1996).

$$\frac{1}{2}\|\mathbf{w}\|^2 + C\sum_i \xi_i \qquad \text{subject to } y_i(\langle \mathbf{w}, \mathbf{x}_i \rangle + b) \geq 1 - \xi_i \qquad \forall_i \xi_i \geq 0 \quad \forall_i \tag{12}$$

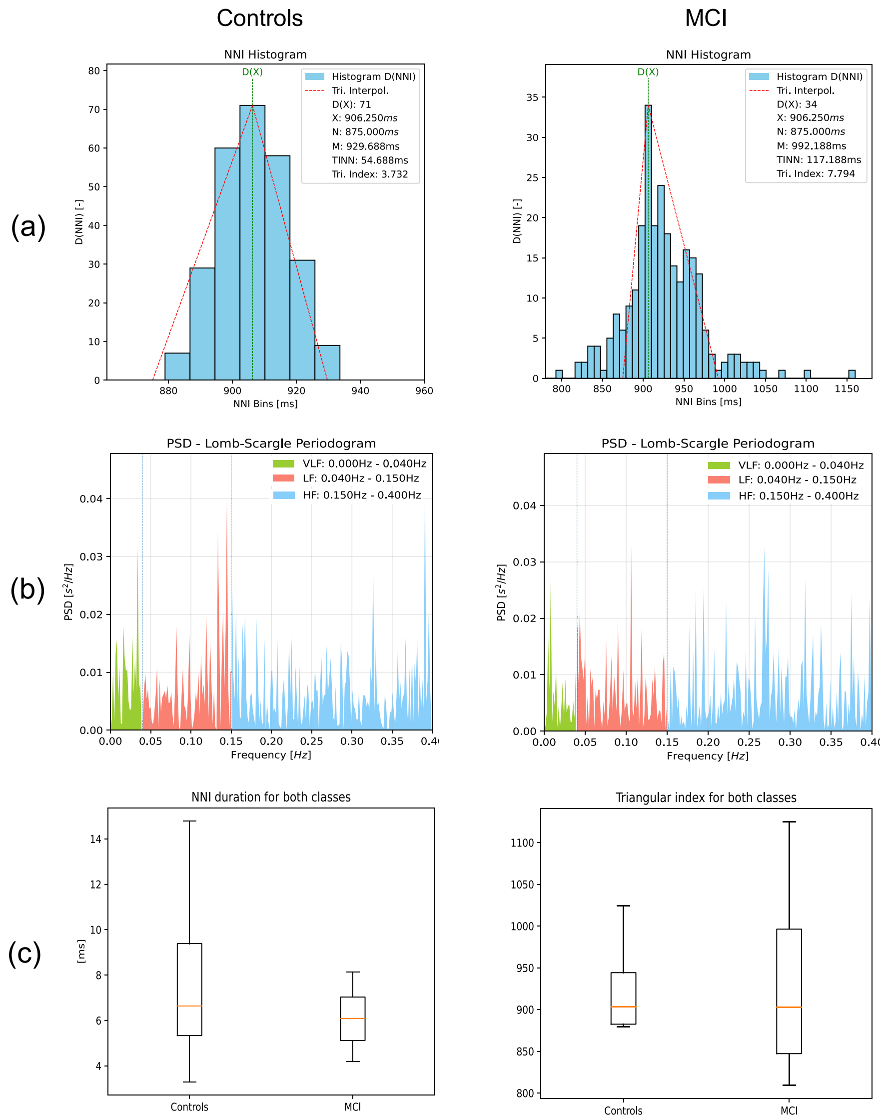

Fig. 2. (a) Average NNI histogram and (b) Power Spectral Density (PSD) for controls (left) and MCI (right). (c) Average NNI duration and Triangular index for both classes.

where C symbolizes the penalty for misclassification. The formula for the solution to this optimization problem is set forth below:

$$\mathbf{w} = \sum_{i=1}^{n} y_i \alpha_i \mathbf{x}_i \tag{13}$$

This formula is derived post the application of the Lagrangian multipliers. By replacing the value of $\mathbf{w}$ from Eq. (11), the decision function can be restated in its dual form as:

$$f(\mathbf{x}i) = \sum i = 1^n \alpha_i K(\mathbf{x}, \mathbf{x}_i) + b \tag{14}$$

Here, the decision function of the classifier is structured around the learning of the coefficients α_i and b. Furthermore, the resemblance between samples $\mathbf{x}$ and $\mathbf{x}_i$ is gauged through the utilization of the kernel function $K(\mathbf{x}, \mathbf{x}_i)$.

Fig. 3 includes a schematic representation of the pipeline proposed in our method. The NNI are computed from the peaks of the original ECG signals. Differences between consecutive NNI are calculated, excluding those which are considered as outliers. Then, features from different domains are computed from the resulting NNI to summarize the information contained in each one of them. Given the high number of the resulting variables, a PCA is performed to reduce the dimensionality. We selected this method given the high performance and simplicity show in literature. The number of components used in classification was derived from those that preserve the 90% of the overall variance. Finally, they are entered into an SVM classifier to perform the classification stage. The election of this classifier was done in order to strike a balance between performance and robustness.

3.7. Performance evaluation

For evaluating the model's ability to generalize and to avoid overfitting, it is of extreme importance to test its performance on data it has not seen before. Overfitting is a potential risk when the model's complexity is too elevated and it aligns itself well only to the data it was trained on. To counteract this, a k-fold cross-validation method, as proposed by Kohavi (1995), was put into practice to divide the entire dataset into training and testing subsets. The model only uses the first subset for training, and its performance was examined using the test subset. This iterative procedure was repeated five times (5-fold scheme), implying that the final performance was an average of the outcomes from each individual fold. This performance was evaluated using a range of metrics extrapolated from the confusion matrix, as

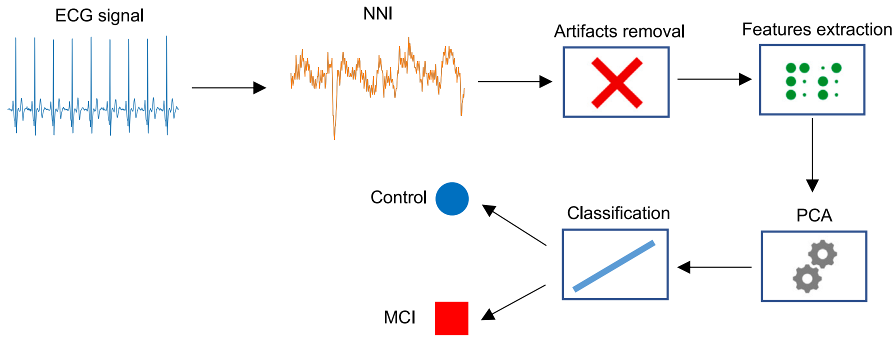

Fig. 3. Diagram of the framework used. The NNI are computed from the ECG signal, and features from different domains are extracted. Then, PCA projects these features into a new space, and the resulting ones that remain a 90% of variance are entered into an SVM classifier. This algorithm reveals the diagnosis (control or MCI) of each subject.

detailed below:

$$Bal\ Acc = \frac{1}{2}\left(\frac{TP}{P} + \frac{TN}{N}\right) \qquad Prec = \frac{T_P}{T_P+F_P}$$

$$Sens = \frac{T_P}{T_P+F_N} \qquad Spec = \frac{T_N}{T_N+F_P}$$

$$F1-score = \frac{2 \cdot Prec \cdot Sens}{Prec+Sens} \qquad AUC = \frac{1}{2}\left(\frac{TP}{P} + \frac{TN}{N}\right)$$

The experiments conducted in this research aimed at discerning differences in the HRV signal between CTL and MCI patients. In this scenario, True positives (TP) represent the count of correctly classified MCI patients, while true negatives (TN) refer to correctly identified controls. False positives (FP) signify the count of controls erroneously labeled as MCI patients, and false negatives (FN) refer to the MCI patients wrongly identified as controls. In addition, the area under the receiver operating characteristic curve (AUC) was utilized as an auxiliary metric to assess the model's capability to differentiate between classes (Hajian-Tilaki, 2013; Mandrekar, 2010).

After the computation of the classifier's performance, it is important to evaluate its statistical significance. We followed a scheme based on non-parametric permutation tests (Golland & Fischl, 2003). This technique involves shuffling the labels linked with each ECG signal before performing the classification. This process was repeated 10,000 times to assemble an empirical accuracy distribution. The likelihood of a specific accuracy was determined by comparing the resulting scores when training the classifier with correct labels and the empirical distribution (North, Curtis, & Sham, 2002). This probability can be summarized by the p-value, as shown below:

$$p = \frac{n+1}{N+1} \tag{15}$$

where n denotes the count of instances where the precision achieved exceeded the true precision, while N indicates the total number of permutations employed in creating the empirical distribution. A result is deemed statistically significant if it falls below the predefined significance threshold, commonly set at $p = 0.05$.

4. Experimental setup

The experiments performed in this study can be summarized as an exploratory analysis aimed at investigating the relationship between the cognitive state of an individual and their HRV signals. The primary objective was to assess the existence of distinct information in HRV signals between controls and patients with MCI. We evaluate the performance of the complete classification pipeline, in addition to measure the results obtained when PCA is not applied to evaluate its influence in the performance. Thus, the different analysis performed are:

- **Classification between CTL and MCI patients** to evaluate differences in their HRV by using the complete system proposed.
- **Influence in performance of the feature extraction technique and classification algorithm.** Specifically, three different kernels for the SVM classifier were employed: linear, polynomial and Radial Basis Function (RBF), in addition to a Random Forest (RF) classifier (Breiman, 2001) to evaluate the performance of another traditional algorithm. The first two were used in combination with PCA (feature extraction) and all of them with SVM (classification).
- **Results interpretation through the measurement of the contribution of each independent variable**. Evaluation of the loadings of each component to rank all variables according to their informativeness.
- **Evaluation of the statistical significance of the results obtained.** To do so, we performed permutation testing to build an empirical accuracy distribution and compare it with the accuracy obtained when no permutation is applied.

In all experiments, the parameters associated with the different kernels were optimized by using a grid search within a 5-fold cross-validation procedure. This means that the train subset was subdivided into two partitions: one for training the model and another for evaluating the performance. Specifically, we focused on the cost (C) and gamma (γ) parameters associated with SVM, as well as the degree of the polynomial. The optimum value for C and γ was selected from the range 10^{-5} to 10^{5} in steps of 10, whereas the degree of the polynomial ranged from 2 to 3. With reference to the RF classifier, two parameters were optimized: the number of trees of the forest (from the range 2 to 10) and the maximum depth of the tree (from 1 to 5). The values that led to the best results were finally employed in the model used in the test set. The experiments conducted employed pyHRV software (Gomes et al., 2019) and custom code written in Python 3.6. Besides, a number of additional libraries was used, such as PyTorch 1.12.1 and Numpy 1.23.5. The experiments were carried out on a cluster with the following hardware specifications: two Intel® Xeon® E5-2630 node 2.40 GHz processors, with 10 cores per processor. Besides, the total RAM memory capacity of the system is 128 GB.

5. Results

Initially, we assessed the classification performance between CTL and MCI patients without applying any dimensionality reduction. In this case, the features computed during the preprocessing based on different domains (time, frequency, etc.) were used as inputs of the SVM classifier, leading to a balanced accuracy of 61.85% and an AUC = 0.63. As presented in Table 5, our method outperformed the baseline approach with significantly higher balanced accuracy (75.01%) and AUC (0.80), highlighting the need of reducing the dimensionality prior to classification. In fact, the projection provided by the principal components allows the classifier to find an optimum solution for separating the two classes. Fig. 4 shows a representation of the samples associated

Table 5
Performance obtained in the experiments conducted. Different kernels were employed both in feature extraction and classification stages: linear, polynomial and RBF. On the other hand, no feature extraction was performed in the baseline approach. RF refers to random forest classifier.

CTL *vs* MCI	Bal Acc (%)	Sens (%)	Spec (%)	Prec (%)	AUC	F1-score (%)
Baseline	61.85 ± 9.72	59.05 ± 16.27	61.92 ± 24.32	63.49 ± 18.02	0.63 ± 0.16	61.14 ± 11.60
PCA + Linear	71.67 ± 12.76	66.67 ± 17.57	76.67 ± 12.09	77.00 ± 17.12	0.72 ± 0.12	68.95 ± 16.80
PCA + RBF	65.83 ± 12.47	53.59 ± 19.65	83.33 ± 13.94	75.00 ± 19.02	0.66 ± 0.12	56.15 ± 18.28
PCA + Poly (2)	69.17 ± 6.23	**73.33 ± 22.61**	65.00 ± 18.98	72.00 ± 14.23	0.69 ± 0.08	69.10 ± 7.85
PCA + RF	71.08 ± 6.37	72.61 ± 23.71	63.88 ± 18.76	72.03 ± 14.65	0.67 ± 0.08	68.36 ± 7.98
KPCA + Linear	72.50 ± 11.47	61.67 ± 16.82	83.33 ± 13.99	80.00 ± 18.71	0.73 ± 0.12	65.29 ± 18.55
KPCA + RBF	**75.01 ± 12.36**	66.67 ± 17.12	**87.33 ± 13.94**	**80.00 ± 18.71**	**0.80 ± 0.11**	**70.62 ± 16.9**
KPCA + Poly (3)	71.67 ± 13.28	65.00 ± 18.86	78.33 ± 15.43	76.00 ± 17.14	0.72 ± 0.11	67.68 ± 18.18
KPCA + RF	72.38 ± 10.55	62.32 ± 16.04	81.89 ± 13.46	79.17 ± 18.26	0.73 ± 0.15	65.11 ± 17.34

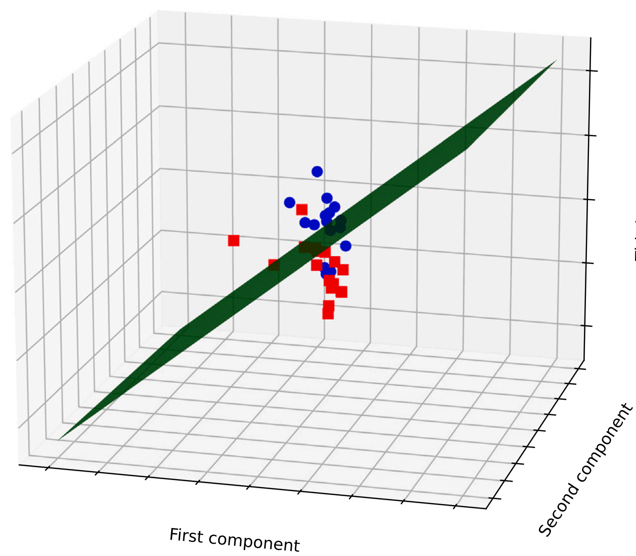

Fig. 4. Representation of the three principal components obtained for all the patients in the database and the decision surface from the linear SVM classifier. The hyperplane allows the correct separation between Controls and MCI patients.

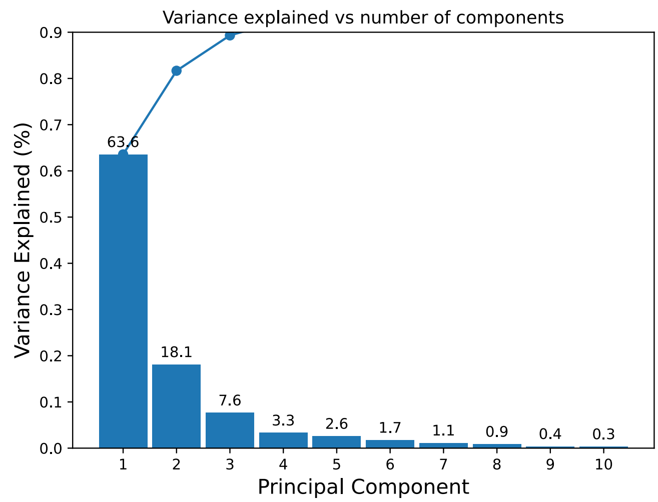

Fig. 5. Relation between the percentage of variance explained and the number of components. The first four principal components account for 90% of the total variance.

with both diagnosis and the hyperplane that allows the distinction between them.

Results clearly manifest that PCA improves the system's performance, but it is important to note that they are better when a non-linear kernel was used regardless of the kernel of the SVM classifier. Specifically, the AUC ranges from 0.72 to 0.80 in this scenario, whereas the values obtained when using a classical version of PCA are contained in the range [0.66 – 0.72]. With reference to the SVM classifier, the best results were obtained when the RBF kernel was applied. This case outperforms the other alternatives in most of metrics, as Table 5 shows, yielding a balanced accuracy of 75.01%.

In addition to improve the model's performance, PCA allows expanding our knowledge about the informativeness of each individual variable. As explained in previous sections, only the resulting components that preserve 90% of the total variance were used in the classification stage. It can be seen in the example showed in Fig. 5 that the first four principal components explain more than 90% of the variance of the original data. In fact, most of the information is contained in the two first components, which demonstrates that using a small number of features in the transformed space can be enough to get a large classification performance. Besides, it is possible to analyze the contribution of each individual feature to each principal component. With reference to the first one, there are five variables that contribute almost equally (see Fig. 6). This behavior is similar than in the second component, but in the third one there is a higher variability in the loadings of the different features. It is also important to remark the nature of the HRV measurements. In the first component, most of them are time-domain features (CVNNI, RMSSD, SDSD, SDNN), whereas in the second one frequency- and non-linear measurements appear. Finally, the third component contains a much more heterogeneous sample, with time-domain, frequency-domain and non-linear measurements.

It is clear that our findings indicate that MCI patients exhibit distinct HRV patterns compared to controls, as evidenced by the excellent diagnostic accuracy achieved by our classifier. Thus, the remarkable performance observed across all evaluation metrics further validates the effectiveness of our proposed method. This superiority also appears in the area under the ROC curve, as depicted in Fig. 7. This graphical representation clearly illustrates the superior performance of our framework. Lastly, Fig. 8 showcases the empirical distributions obtained through label shuffling in a permutation process, alongside the accuracy achieved when classifying with correct labels. The evident significance of the results supports the validity of our findings from a statistical perspective.

6. Discussion

This study introduces a classification framework aimed at investigating HRV variations related to the cognitive state of patients. The methodology involves employing signal processing techniques to extract features from multiple domains, including time, frequency and non-linear ones. These features are then subjected to PCA, which facilitates dimensionality reduction while preserving the underlying information. The resulting components that preserve 90% of the total variance are utilized as inputs for an SVM classifier, which establishes a hyperplane to differentiate samples belonging to the two classes: MCI and controls. We assessed the performance of this approach using various metrics and examined the potential of HRV as an early indicator in the progression of MCI.

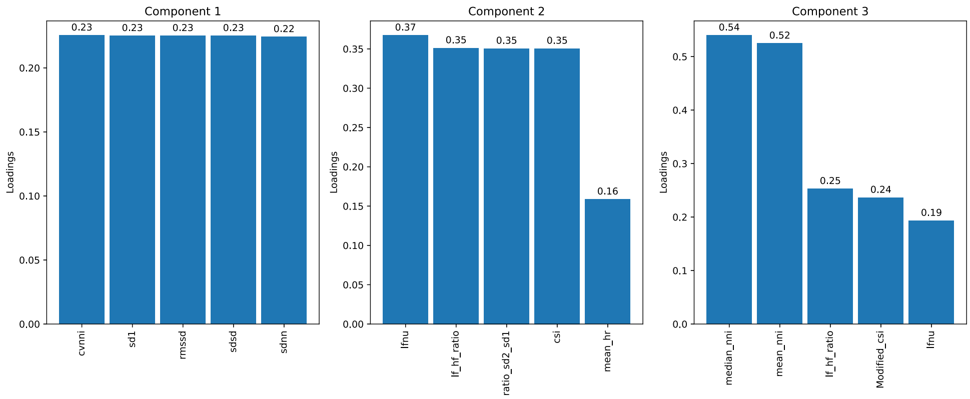

Fig. 6. Contribution of each individual feature to the first three principal components. Time-domain features are more related to the first component, whereas frequency-domain features emerge in the second one. The third component includes a wide range of variables including time- and frequency-domain, as well as non-linear ones.

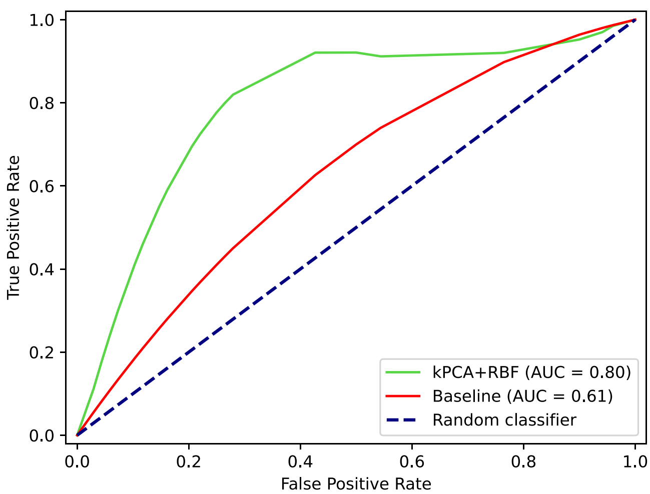

Fig. 7. ROC curves obtained in the classification between controls and MCI patients. These representations demonstrate the superior performance of the proposed method over the baseline one.

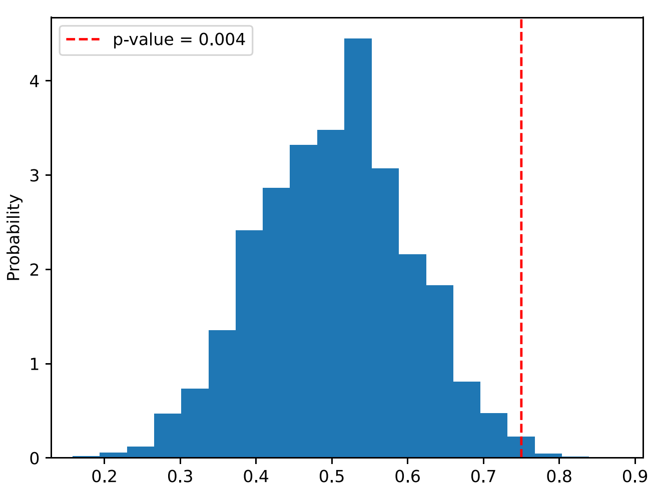

Fig. 8. Distribution obtained once applied the permutations scheme. Performance derived from the actual labels are depicted by the vertical red line.

The classification framework proposed in this study demonstrates a high performance, which is beneficial for investigating the relationship between HRV signals and cognitive decline. Although the primary objective was not classification, it is noteworthy that a high accuracy rate of 75.01% was achieved. Previous studies have proposed a correlation between HRV and cognitive function, and some studies have explored the physiological mechanisms that connect them (Forte et al., 2019). However, the findings are inconclusive due to conflicting opinions. For example, the high-frequency bands in the HRV spectrum correspond to parasympathetic cardiac activity, and a reduction in these bands may suggest an inability to respond to changing demands (Reyes Del Paso, González, Hernández, Duschek, & Gutiérrez, 2009). Some hypotheses suggest that the same brain regions are involved in both self-regulatory systems and cardiac autonomic activity (Ellis & Thayer, 2010; Thayer, Åhs, Fredrikson, Sollers, & Wager, 2012). Low LF-HRV has been associated with the risk of developing cognitive impairment, possibly because it is linked to white matter lesions in MCI or AD patients (De Vilhena Toledo & Junqueira, 2008; Galluzzi et al., 2009). Alterations in HRV have been detected in MCI patients, suggesting that autonomic dysfunctions may precede the onset of cognitive impairment (Kong et al., 2020). Although many studies suggest a correlation between HRV and cognitive impairment, the connection between them is not yet fully understood. The main contribution of the exploratory analysis conducted in this work is that we have found clear differences between the HRV signals associated with controls and MCI patients. In fact, our results based on artificial intelligence corroborate the potential role of ECG signals as a marker of the cognitive decline.

In this exploratory analysis, it is worth noting that the selection of variables affecting performance is entirely data-driven. For instance, the features were computed using a similar pipeline as described in the literature. However, instead of using these features directly as input to the classification algorithm, we employed a feature extraction methodology to obtain a new set of variables. This approach optimizes variable selection based on their importance, measured by the variance they represent in the new subspace. By doing so, we mitigate individual biases that could impact the results. The size of the dataset also plays a significant role in our findings. As expected, a larger number of patients contributes to more robust results. For our study, we used a database comprising 36 subjects, which is comparable to or slightly smaller than the sample sizes used in previous studies (Colzato & Steenbergen, 2017; Ferdinando, Seppänen, & Alasaarela, 2016; Lucena, Barros, Takeuchi, & Ohnishi, 2009; Lyle et al., 2017; Ottaviani et al., 2019; Rogers, Schaffarczyk, Clauß, Mourot, & Gronwald, 2022). However, we employed different mechanisms to address potential biases in constructing the machine learning model. Firstly, we used balanced accuracy as a performance metric for the algorithm. This choice ensures that the majority class (the MCI) does not dominate the training of the model. Secondly, we assessed the significance of our results to verify their statistical relevance. We conducted a high number of permutations

(10,000) and obtained a small p-value ($p = 0.006$), confirming the validity of our findings and minimizing the potential bias.

We have developed a complete framework capable of detecting MCI patients from ECG data. It is important to note the high performance that our method yields: and accuracy and an AUC of 75.01% and 0.8, respectively. Previous studies have demonstrated the existence of biomarkers for an early detection of a cognitive decline. However, most of them are based on data extracted from common brain imaging or neuropsychological tests (Arco, Ramírez, Puntonet, Górriz, & Ruz, 2016; Bottani et al., 2023; Chagué et al., 2021; Jiménez-Mesa et al., 2023; Lampe et al., 2023; Zubrikhina et al., 2023). For this reason, demonstrating that HRV signals also contain this kind of information is extraordinarily relevant. Besides, it is important to note that ECG acquisition is much less invasive than other neuroimaging approaches, which facilitates the data acquisition. Moreover, the equipment is much more affordable than the scanners needed for imaging acquisition, which are not present in all clinical centers given their high price. On the other hand, ECG equipments are more widespread, allowing our method to be used in environments of any socioeconomic range.

Finally, it is important to remark that our work paves the way for future studies that evaluate potential factors related to the human cognitive decline. This is especially relevant when studying the behavior of variables that are not usually related to a specific pathology. For example, the analysis of ECG signals is commonly performed when evaluating cardiac pathologies, and not cognitive disorders. Recent advances support our findings that information about the cognitive health is present not only in the result of psychological tests or medical imaging, but also in the brainwaves of sleep (Adra et al., 2023) or in genetic risk factors (Duan et al., 2023). The complexity in the study of this kind of signals requires the development of intelligent systems that provide not only accurate solutions but explainable ones that allow clinicians to improve the human healthcare (Calisto, Ferreira, Nascimento, & Gonçalves, 2017; Calisto et al., 2020).

7. Conclusion

In this study, we present an intelligent system designed to assess clinical disparities using ECG signals. These differences can be derived from HRV, which measures the variation in beat-to-beat intervals over a specific time period. After preprocessing the data to eliminate artifacts, we compute features from various domains to enhance the method's robustness. The resultant features are then projected onto a new space using PCA, with the most significant contributors to the variance being selected for input into an SVM classifier. This approach achieves a 75.01% accuracy rate in distinguishing between control subjects and those with MCI as well as an AUC value of 0.80. These results indicate the presence of changes in ECG signals that can be associated with cognitive decline. Additionally, this work paves the way for future research into AI-based algorithms for the study of different biomedical signals. Finally, our findings demonstrate the potential of HRV as an early indicator of dementia, which is especially valuable considering its cost-effectiveness compared to different neuroimaging modalities. These results pave the way for future studies to evaluate potential factors associated with the human cognitive decline that are not commonly taken into account. Besides, our methodology offers a practical solution for the identification of future events that can be related to variables in a previous point in time. A deeper research in this topic could expand our knowledge not only about the occurrence (or not) of the event, but informs us about when a specific pathology is going to happen. This is particularly interesting in clinical environments where the treatment must begin in an exact instant to strike a balance between risk and benefit: soon enough to avoid the appearance of the disease but not too soon to decrease the probability of a side effect associated with the treatment.

Funding

This work was supported by projects PID2022-137461NB-C32 (Spanish "Ministerio de Ciencia e Innovación, /AEI /10.13039/501100 011033/ FEDER, UE), UMA20-FEDERJA-086 European Regional Development Funds (ERDF) "Una manera de hacer Europa", and by Spanish "Ministerio de Universidades" (Next Generation EU funds) through Margarita-Salas grant to J.E. Arco. Funding for open access charge was provided by Universidad de Málaga / CBUA.

CRediT authorship contribution statement

Juan E. Arco: Conceptualization, Methodology, Software, Investigation, Writing – original draft. **Nicolás J. Gallego-Molina:** Methodology, Investigation, Writing – original draft. **Andrés Ortiz:** Conceptualization, Methodology, Investigation, Writing – original draft. **Katy Arroyo-Alvis:** Conceptualization, Investigation, Methodology. **P. Javier López-Pérez:** Conceptualization, Investigation, Methodology.

Declaration of competing interest

The authors declare that they have no known competing financial interests or personal relationships that could have appeared to influence the work reported in this paper.

Data availability

The authors do not have permission to share data.

References

Abou-Abbas, L., Henni, K., Jemal, I., Mitiche, A., & Mezghani, N. (2023). Patient-independent epileptic seizure detection by stable feature selection. *Expert Systems with Applications*, Article 120585.

Adra, N., Dümmer, L., Paixao, L., Tesh, R., Sun, H., Ganglberger, W., et al. (2023). Decoding information about cognitive health from the brainwaves of sleep. *Scientific Reports*, *13*, 1–14. http://dx.doi.org/10.1038/s41598-023-37128-7.

Alessio, S. M. (2006). Discrete wavelet transform (DWT). In *Encyclopedia of multimedia* (pp. 645–714).

Alizadehsani, R., Sharifrazi, D., Izadi, N. H., Joloudari, J. H., Shoeibi, A., Gorriz, J. M., et al. (2021). Uncertainty-aware semi-supervised method using large unlabeled and limited labeled COVID-19 data. *ACM Transactions on Multimedia Computing, Communications, and Applications*, *17*(3s).

Allan, L., Kerr, S., Ballard, C., Allen, J., Murray, A., McLaren, A., et al. (2005). Autonomic function assessed by heart rate variability is normal in Alzheimer's disease and vascular dementia. *Dementia and geriatric cognitive disorders*, *19*, 140–144.

Arco, J. E., Ortiz, A., Castillo-Barnes, D., Górriz, J. M., & Ramírez, J. (2022). Quantifying inter-hemispheric differences in Parkinson's disease using siamese networks. In J. M. Ferrández Vicente, J. R. Álvarez-Sánchez, F. de la Paz López, & H. Adeli (Eds.), *Artificial intelligence in neuroscience: affective analysis and health applications* (pp. 156–165). Springer International Publishing.

Arco, J. E., Ortiz, A., Castillo-Barnes, D., Górriz, J. M., & Ramírez, J. (2023). Ensembling shallow siamese architectures to assess functional asymmetry in Alzheimer's disease progression. *Applied Soft Computing*, *134*, Article 109991.

Arco, J. E., Ortiz, A., Gallego-Molina, N. J., Górriz, J. M., & Ramírez, J. (2023). Enhancing multimodal patterns in neuroimaging by siamese neural networks with self-attention mechanism. *International Journal of Neural Systems*, *33*(4), Article 2350019.

Arco, J. E., Ortiz, A., Ramírez, J., Martínez-Murcia, F. J., Zhang, Y.-D., Broncano, J., et al. (2022). Probabilistic combination of non-linear eigenprojections for ensemble classification. *IEEE Transactions on Emerging Topics in Computational Intelligence*, *7*, 1–11.

Arco, J. E., Ortiz, A., Ramírez, J., Martínez-Murcia, F. J., Zhang, Y.-D., & Górriz, J. M. (2023). Uncertainty-driven ensembles of multi-scale deep architectures for image classification. *Information Fusion*, *89*, 53–65.

Arco, J. E., Ramírez, J., Górriz, J. M., & Ruz, M. (2021). Data fusion based on searchlight analysis for the prediction of Alzheimer's disease. *Expert Systems with Applications*, *185*, Article 115549.

Arco, J. E., Ramírez, J., Puntonet, C. G., Górriz, J. M., & Ruz, M. (2016). Improving short-term prediction from MCI to AD by applying searchlight analysis. In *2016 IEEE 13th international symposium on biomedical imaging* (pp. 10–13).

Bach, F., & Jordan, M. (2003). Kernel independent component analysis. In *2003 IEEE international conference on acoustics, speech, and signal processing, 2003. proceedings, vol. 4* (pp. IV–876).

Barrero, F., Vives, F., & Morales, B. (2006). Evaluación de la versión española del Memory Impariment Screen. *Revista de Neurología*, *43*(1), 15–19.

Behbahani, S., Jafarnia Dabanloo, N., & Motie Nasrabadi, A. (2013). Ictal heart rate variability assessment with focus on secondary generalized and complex partial epileptic seizures. *Advances in Bioresearch*, *4*, 50–58.

Beniczky, S., Karoly, P., Nurse, E., Ryvlin, P., & Cook, M. (2021). Machine learning and wearable devices of the future. *Epilepsia*, *62*(S2), S116–S124.

Benton, A. (1974). *Revised visual retention test* (fourth ed.). New York: Psychological Corporation.

Benton, A. (1983). *Contributions to neuropsychological assessment: A clinical manual*. Oxford Medicine Publications.

Bhardwaj, D., Jutai, J., & Fallavollita, P. (2023). Chapter 9 - role of smart technologies in detecting cognitive impairment and enhancing assisted living. In A. El Saddik (Ed.), *Digital twin for healthcare* (pp. 181–193). Academic Press.

Bhaskar, R., & Ghatak, S. K. (2013). Nonlinear methods to assess changes in heart rate variability in type 2 diabetic patients. *Arquivos Brasileiros de Cardiologia*, *101*, 317–327.

Boissoneault, J., Letzen, J., Robinson, M., & Staud, R. (2019). Cerebral blood flow and heart rate variability predict fatigue severity in patients with chronic fatigue syndrome. *Brain Imaging and Behavior*, *13*, 789–797.

Boser, B., Guyon, I., & Vapnik, V. (1996). A training algorithm for optimal margin classifier. In *Proceedings of the fifth annual ACM workshop on computational learning theory, vol. 5*.

Bosl, W. J., Leviton, A., & Loddenkemper, T. (2021). Prediction of seizure recurrence. A note of caution. *Frontiers in Neurology*, *12*.

Bottani, S., Burgos, N., Maire, A., Saracino, D., Ströer, S., Dormont, D., et al. (2023). Evaluation of MRI-based machine learning approaches for computer-aided diagnosis of dementia in a clinical data warehouse. *Medical Image Analysis*, *89*, Article 102903.

Bowie, C., & Harvey, P. (2006). Administration and interpretation of trail making test. *Nature protocols*, *1*, 2277–2281.

Breiman, L. (2001). Random forests. *Machine Learning*, *45*(1), 5–32.

Brennan, M., Palaniswami, M., & Kamen, P. (2001). Do existing measures of Poincare plot geometry reflect nonlinear features of heart rate variability? *IEEE Transactions on Biomedical Engineering*, *48*(11), 1342–1347.

Buchman, T., Stein, P., & Goldstein, B. (2002). Heart rate variability in critical illness and critical care. *Current Opinion in Critical Care*, *8*, 311–315.

Calisto, F. M., Fernandes, J., Morais, M., Santiago, C., Abrantes, J. M., Nunes, N., et al. (2023). Assertiveness-based agent communication for a personalized medicine on medical imaging diagnosis. In *Proceedings of the 2023 CHI conference on human factors in computing systems* (pp. 1–20). New York, NY, USA: Association for Computing Machinery.

Calisto, F. M., Ferreira, A., Nascimento, J. C., & Gonçalves, D. (2017). Towards touch-based medical image diagnosis annotation. In *Proceedings of the 2017 ACM international conference on interactive surfaces and spaces* (pp. 390–395). New York, NY, USA: Association for Computing Machinery.

Calisto, F. M., Nunes, N., & Nascimento, J. C. (2020). BreastScreening: On the use of multi-modality in medical imaging diagnosis. In *Proceedings of the international conference on advanced visual interfaces* (pp. 1–5). New York, NY, USA: Association for Computing Machinery.

Cha, S.-A., Park, Y.-M., Yun, J.-S., Lee, S.-H., Ahn, Y.-B., Kim, S.-R., et al. (2018). Time- and frequency-domain measures of heart rate variability predict cardiovascular outcome in patients with type 2 diabetes. *Diabetes Research and Clinical Practice*, *143*, 159–169.

Chagué, P., Marro, B., Fadili, S., Houot, M., Morin, A., Samper-González, J., et al. (2021). Radiological classification of dementia from anatomical MRI assisted by machine learning-derived maps. *Journal of Neuroradiology*, *48*(6), 412–418.

Chen, C.-W., Kwok, Y.-T., Cheng, Y.-T., Huang, Y.-S., Kuo, T., Wu, C. H., et al. (2023). Reduced slow-wave activity and autonomic dysfunction during sleep precede cognitive deficits in Alzheimer's disease transgenic mice. *Scientific Reports*, 1–17. http://dx.doi.org/10.1038/s41598-023-38214-6.

Chen, W., Liu, G.-Z., Su, S., Jiang, Q., & Nguyen, H. (2017). A CHF detection method based on deep learning with RR intervals. In *Annual international conference of the IEEE engineering in medicine and biology society. IEEE engineering in medicine and biology society. conference, vol. 2017* (pp. 3369–3372).

Chou, Y.-T., Sun, Z.-J., Shao, S.-C., Yang, Y.-C., Lu, F.-H., Chang, C.-J., et al. (2022). Autonomic modulation and the risk of dementia in a middle-aged cohort: A 17-year follow-up study. *Biomedical Journal*.

Coelho, B. F. O., Massaranduba, A. B. R., dos Santos Souza, C. A., Viana, G. G., Brys, I., & Ramos, R. P. (2023). Parkinson's disease effective biomarkers based on Hjorth features improved by machine learning. *Expert Systems with Applications*, *212*, Article 118772.

Colzato, L. S., & Steenbergen, L. (2017). High vagally mediated resting-state heart rate variability is associated with superior action cascading. *Neuropsychologia*, *106*, 1–6.

De Vilhena Toledo, M. A., & Junqueira, L. F., Jr. (2008). Cardiac sympathovagal modulation evaluated by short-term heart interval variability is subtly impaired in Alzheimer's disease. *Geriatrics & Gerontology International*, *8*(2), 109–118.

Deng, X., Liu, E., Li, S., Duan, Y., & Xu, M. (2023). Interpretable multi-modal image registration network based on disentangled convolutional sparse coding. *IEEE Transactions on Image Processing*, *32*(1), 1078–1091.

Duan, H., Zhou, D., Xu, N., Yang, T., Wu, Q., Wang, Z., et al. (2023). Association of unhealthy lifestyle and genetic risk factors with mild cognitive impairment in Chinese older adults. *JAMA Network Open*, *6*(7), e2324031.

Duarte Pedroza, L., Espitia, A., & Montañés, P. (2016). Aportes y limitaciones del Boston naming test: evidencia a partir de controles colombianos. *Acta Neurológica Colombiana*, *32*, 290–296.

Ellis, R. J., & Thayer, J. F. (2010). Music and autonomic nervous system (Dys)function. *Music Perception*, *27*(4), 317–326.

Feng, H., Yang, B., Wang, J., Liu, M., Yin, L., Zheng, W., et al. (2023). Identifying malignant breast ultrasound images using ViT-patch. *Applied Sciences*, *13*(6).

Ferdinando, H., Seppänen, T., & Alasaarela, E. (2016). Comparing features from ECG pattern and HRV analysis for emotion recognition system. In *2016 IEEE conference on computational intelligence in bioinformatics and computational biology, vol. 1* (pp. 1–6).

Florjanski, W., Malysa, A., Orzeszek, S., Smardz, J., Olchowy, A., Paradowska-Stolarz, A., et al. (2019). Evaluation of biofeedback usefulness in masticatory muscle activity management—A systematic review. *Journal of Clinical Medicine*, *8*(6).

Folstein, M. F., Folstein, S. E., & McHugh, P. R. (1975). "Mini-mental state": A practical method for grading the cognitive state of patients for the clinician. *Journal of Psychiatric Research*, *12*(3), 189–198.

Forte, G., Favieri, F., & Casagrande, M. (2019). Heart rate variability and cognitive function: A systematic review. *Frontiers in Neuroscience*, *13*.

Gallego-Molina, N. J., Ortiz, A., Martínez-Murcia, F. J., Formoso, M. A., & Giménez, A. (2022). Complex network modeling of EEG band coupling in dyslexia: An exploratory analysis of auditory processing and diagnosis. *Knowledge-Based Systems*, *240*, Article 108098.

Galluzzi, S., Nicosia, F., Geroldi, C., Alicandri, A., Bonetti, M., Romanelli, G., et al. (2009). Cardiac autonomic dysfunction is associated with white matter lesions in patients with mild cognitive impairment. *The Journals of Gerontology: Series A*, *64A*(12), 1312–1315.

Golland, P., & Fischl, B. (2003). Permutation tests for classification: Towards statistical significance in image-based studies. In C. Taylor, & J. A. Noble (Eds.), *Information processing in medical imaging* (pp. 330–341). Berlin, Heidelberg: Springer Berlin Heidelberg.

Gomes, P., Margaritoff, P., & Silva, H. (2019). pyHRV: Development and evaluation of an open-source python toolbox for heart rate variability (HRV). In *Proc. int'l conf. on electrical, electronic and computing engineering* (pp. 822–828).

Górriz, J., álvarez Illán, I., álvarez Marquina, A., Arco, J., Atzmueller, M., Ballarini, F., et al. (2023). Computational approaches to explainable artificial intelligence: advances in theory, applications and trends. *Information Fusion*, *100*, 101945.

Grant, D., & Berg, E. (1948). A behavioral analysis of degree of reinforcement and ease of shifting to new responses in a Weigl-type card-sorting problem. *Journal of Experimental Psychology*, *38*(4), 404–411.

Hadjem, M., Naït-Abdesselam, F., & Khokhar, A. (2016). ST-segment and T-wave anomalies prediction in an ECG data using RUSBoost. In *2016 IEEE 18th international conference on E-health networking, applications and services, vol. 1* (pp. 1–6).

Haensel, A., Mills, P. J., Nelesen, R. A., Ziegler, M. G., & Dimsdale, J. E. (2008). The relationship between heart rate variability and inflammatory markers in cardiovascular diseases. *Psychoneuroendocrinology*, *33*(10), 1305–1312.

Hajian-Tilaki, K. (2013). Receiver operating characteristic (ROC) curve analysis for medical diagnostic test evaluation. *Caspian Journal of Internal Medicine*, *4*, 627–635.

Hämmerle, P., Eick, C., Blum, S., Schlageter, V., Bauer, A., Rizas, K. D., et al. (2020). Heart rate variability triangular index as a predictor of cardiovascular mortality in patients with atrial fibrillation. *Journal of the American Heart Association*, *9*(15), Article e016075.

Han, S.-J., Xu, Q.-Q., Pan, H., Liu, W.-J., Dai, Q.-Q., Lin, H.-Y., et al. (2023). Network pharmacology and molecular docking prediction, combined with experimental validation to explore the potential mechanism of Qishen Yiqi pills against HF-related cognitive dysfunction. *Journal of Ethnopharmacology*, *314*, Article 116570.

Hillebrand, S., Gast, K. B., de Mutsert, R., Swenne, C. A., Jukema, J. W., Middeldorp, S., et al. (2013). Heart rate variability and first cardiovascular event in populations without known cardiovascular disease: meta-analysis and dose–response meta-regression. *EP Europace*, *15*(5), 742–749.

Hoshi, R. A., Pastre, C. M., Vanderlei, L. C. M., & Godoy, M. F. (2013). Poincaré plot indexes of heart rate variability: Relationships with other nonlinear variables. *Autonomic Neuroscience*, *177*(2), 271–274.

Huikuri, H. V. (1995). Heart rate variability in coronary artery disease. *Journal of Internal Medicine*, *237*(4), 349–357.

Ilias, L., Askounis, D., & Psarras, J. (2023). Multimodal detection of epilepsy with deep neural networks. *Expert Systems with Applications*, *213*, Article 119010.

Jiménez-Mesa, C., Arco, J. E., Valentí-Soler, M., Frades-Payo, B., Zea-Sevilla, M. A., Ortiz, A., et al. (2023). Using explainable artificial intelligence in the clock drawing test to reveal the cognitive impairment pattern. *International Journal of Neural Systems*, *33*(04), Article 2350015.

Jolliffe, I. T. (1986). Principal component analysis and factor analysis. In *Principal component analysis* (pp. 115–128). Springer New York.

Khedher, L., Ramírez, J., Górriz, J. M., Brahim, A., & Segovia, F. (2015). Early diagnosis of Alzheimer's disease based on partial least squares, principal component analysis and support vector machine using segmented MRI images. *Neurocomputing*, *151*, 139–150.

Kohavi, R. (1995). A study of cross-validation and bootstrap for accuracy estimation and model selection. In *Proceedings of the 14th international joint conference on artificial intelligence - volume 2* (pp. 1137–1143). San Francisco, CA, USA: Morgan Kaufmann Publishers Inc.

Kong, S. D. X., Hoyos, C. M., Phillips, C. L., McKinnon, A. C., Lin, P., Duffy, S. L., et al. (2020). Altered heart rate variability during sleep in mild cognitive impairment. *Sleep*, *44*(4).

Kristal-Boneh, E., Raifel, M., Froom, P., & Ribak, J. (1995). Heart rate variability in health and disease. *Scandinavian Journal of Work, Environment & Health*, *21*(2), 85–95.

Lampe, L., Huppertz, H.-J., Anderl-Straub, S., Albrecht, F., Ballarini, T., et al. (2023). Multiclass prediction of different dementia syndromes based on multi-centric volumetric MRI imaging. *NeuroImage: Clinical*, *37*, Article 103320.

Lezak, M., Howieson, D., Loring, D., Hannay, H., & Fischer, J. (2004). *Neuropsyhological assesment* (fourth ed.). Oxford University Press.

Li, H., Yuan, D., Wang, Y., Cui, D., & Cao, L. (2016). Arrhythmia classification based on multi-domain feature extraction for an ECG recognition system. *Sensors*, *16*(10).

Liao, D., Cai, J., Brancati, F. L., Folsom, A., Barnes, R. W., Tyroler, H. A., et al. (1995). Association of vagal tone with serum insulin, glucose, and diabetes mellitus — The ARIC study. *Diabetes Research and Clinical Practice*, *30*(3), 211–221.

Lippman, N., Stein, K. M., & Lerman, B. B. (1993). Nonlinear predictive interpolation: a new method for the correction of ectopic beats for heart rate variability analysis. *Journal of Electrocardiology*, *26*(Supplement), S14–S19.

Lippman, N., Stein, K. M., & Lerman, B. B. (1994). Comparison of methods for removal of ectopy in measurement of heart rate variability. *American Journal of Physiology-Heart and Circulatory Physiology*, *267*(1), 411–418.

López, M., Ramírez, J., Górriz, J. M., Illan, I., Salas-Gonzalez, D., Segovia, F., et al. (2009). SVM-based CAD system for early detection of the alzheimer's disease using kernel PCA and LDA. *Neuroscience Letters*, *464*, 233–238.

López, M., Ramírez, J., Górriz, J. M., Salas-Gonzalez, D., Álvarez, I., Segovia, F., et al. (2009). Automatic tool for Alzheimer's disease diagnosis using PCA and Bayesian classification rules. *Electronics Letters*, *45*, 389–391.

Lotufo, P. A., Valiengo, L., Benseñor, I. J. M., & Brunoni, A. R. (2012). A systematic review and meta-analysis of heart rate variability in epilepsy and antiepileptic drugs. *Epilepsia*, *53*.

Lucena, F., Barros, A. K., Takeuchi, Y., & Ohnishi, N. (2009). Heart instantaneous frequency based estimation of HRV from blood pressure waveforms. *IEICE Transactions on Information and Systems*, *E92.D*(3), 529–537.

Lv, Z.-H., Yu, Z., Xie, S., & Alamri, A. (2022). Deep learning-based smart predictive evaluation for interactive multimedia-enabled smart healthcare. *ACM Transactions on Multimedia Computing, Communications, and Applications (TOMM)*, *18*, 1–20.

Lyle, J. V., Charlton, P. H., Bonet-Luz, E., Chaffey, G., Christie, M., Nandi, M., et al. (2017). Beyond HRV: Analysis of ECG signals using attractor reconstruction. In *2017 computing in cardiology* (pp. 1–4).

Mandrekar, J. N. (2010). Receiver operating characteristic curve in diagnostic test assessment. *Journal of Thoracic Oncology*, *5*(9), 1315–1316.

Mccraty, R., & Shaffer, F. (2015). Heart rate variability: New perspectives on physiological mechanisms, assessment of self-regulatory capacity, and health risk. *Global Advances in Health and Medicine*, *4*(1), 46–61.

Morris, J., & Samad, T. (2021). Multiscale multivariate statistical process control. In *Encyclopedia of systems and control* (pp. 1396–1402). Springer International Publishing.

Murat, F., Sadak, F., Yildirim, O., Talo, M., Murat, E., Karabatak, M., et al. (2021). Review of Deep Learning-Based Atrial Fibrillation Detection Studies. *International Journal of Environmental Research and Public Health*, *18*(21).

Nezamabadi, K., Sardaripour, N., Haghi, B., & Forouzanfar, M. (2023). Unsupervised ECG analysis: A review. *IEEE Reviews in Biomedical Engineering*, *16*(1), 208–224.

Nicolini, P., Ciulla, M. M., Malfatto, G., Abbate, C., Mari, D., Rossi, P. D., et al. (2014). Autonomic dysfunction in mild cognitive impairment: Evidence from power spectral analysis of heart rate variability in a cross-sectional case-control study. *PLoS One*, *9*(5), 1–15.

Nicolini, P., Lucchi, T., Abbate, C., Inglese, S., Tomasini, E., Mari, D., et al. (2022). Autonomic function predicts cognitive decline in mild cognitive impairment: Evidence from power spectral analysis of heart rate variability in a longitudinal study. *Frontiers in Aging Neuroscience*, *14*.

North, B., Curtis, D., & Sham, P. (2002). A note on the calculation of empirical P values from Monte Carlo procedures. *American Journal of Human Genetics*, *71*, 439–441.

O'Brien, P. D., Hinder, L. M., Callaghan, B. C., & Feldman, E. L. (2017). Neurological consequences of obesity. *The Lancet Neurology*, *16*(6), 465–477.

Ottaviani, C., Zingaretti, P., Petta, A. M., Antonucci, G., Thayer, J. F., & Spitoni, G. F. (2019). Resting heart rate variability predicts inhibitory control above and beyond impulsivity. *Journal of Psychophysiology*, *33*(3), 198–206.

Ranpuria, R., Hall, M., Chan, C. T., & Unruh, M. (2007). Heart rate variability (HRV) in kidney failure: measurement and consequences of reduced HRV. *Nephrology Dialysis Transplantation*, *23*(2), 444–449.

Raudys, S., & Jain, A. (1991). Small sample size effects in statistical pattern recognition: Recommendations for practitioners. *IEEE Transactions on Pattern Analysis and Machine Intelligence*, *13*, 252–264.

Rey, A. (1941). L'examen psychologique dans les cas d'encéphalopathie traumatique. (Les problems). In *Archives de psychologie* (pp. 215–285).

Rey, A. (2009). *Publicaciones de psicología aplicada, REY, Test de copia y de reproducción de memoria de figuras geométricas complejas*. TEA Ediciones, S.A..

Reyes Del Paso, G. A., González, M. I., Hernández, J. A., Duschek, S., & Gutiérrez, N. (2009). Tonic blood pressure modulates the relationship between baroreceptor cardiac reflex sensitivity and cognitive performance. *Psychophysiology*, *46*(5), 932–938.

Rodríguez-Rodríguez, I., Ortiz, A., Gallego-Molina, N. J., Formoso, M. A., & Woo, W. L. (2023). EEG interchannel causality to identify source/sink phase connectivity patterns in developmental dyslexia. *International Journal of Neural Systems*, *33*(04), Article 2350020.

Rogers, B., Schaffarczyk, M., Clauß, M., Mourot, L., & Gronwald, T. (2022). The movesense medical sensor chest belt device as single channel ECG for RR interval detection and HRV analysis during resting state and incremental exercise: A cross-sectional validation study. *Sensors*, *22*(5).

Rovere, M. T. L., Maestri, R., & Pinna, G. D. (2011). Baroreflex sensitivity assessment - latest advances and strategies. *European Cardiology*, *7*(2), 89–92.

Rubin, J., Abreu, R., Ahern, S., Eldardiry, H., & Bobrow, D. (2016). Time, frequency & complexity analysis for recognizing panic states from physiologic time-series. In *PervasiveHealth '16: Proceedings of the 10th EAI international conference on pervasive computing technologies for healthcare* (pp. 81–88). ACM.

Schaich, C. L., Malaver, D., Chen, H., Shaltout, H. A., Hazzouri, A. Z. A., Herrington, D. M., et al. (2020). Association of heart rate variability with cognitive performance: The multi-ethnic study of atherosclerosis. *Journal of the American Heart Association*, *9*(7), Article e013827.

Schölkopf, B., Smola, A., & Müller, K. (1998). Nonlinear component analysis as a kernel eigenvalue problem. *Neural Computation*, *10*(5), 1299–1319.

Seiffert, C., Khoshgoftaar, T. M., Hulse, J. V., & Napolitano, A. (2010). RUSboost: A hybrid approach to alleviating class imbalance. *IEEE Transactions on Systems, Man, and Cybernetics - Part A: Systems and Humans*, *40*, 185–197.

Shaffer, F., & Ginsberg, J. P. (2017). An overview of heart rate variability metrics and norms. *Frontiers in Public Health*, *5*.

Sigcha, L., Borzí, L., Amato, F., Rechichi, I., Ramos-Romero, C., Cárdenas, A., et al. (2023). Deep learning and wearable sensors for the diagnosis and monitoring of Parkinson's disease: A systematic review. *Expert Systems with Applications*, *229*, Article 120541.

Štajner, S., Saggion, H., & Ponzetto, S. P. (2019). Improving lexical coverage of text simplification systems for Spanish. *Expert Systems with Applications*, *118*, 80–91.

Stroop, J. (1935). Studies of interference in serial verbal reactions. *Journal of Experimental Psychology: General*, *18*, 643–662.

Sun, L., Zhang, M., Wang, B., & Tiwari, P. (2023). Few-shot class-incremental learning for medical time series classification. *IEEE Journal of Biomedical and Health Informatics*, *1*(1), 1–11. http://dx.doi.org/10.1109/JBHI.2023.3247861.

Szegedy, C., Liu, W., Jia, Y., Sermanet, P., Reed, S., Anguelov, D., et al. (2015). Going deeper with convolutions. In *2015 IEEE conference on computer vision and pattern recognition, vol. 1* (pp. 1–9).

Tarvainen, M. P., Niskanen, J.-P., & Lipponen, J. (2014). Kubios HRV–heart rate variability analysis software. *Computer Methods and Programs in Biomedicine*, *113*(1), 210–220.

Task Force of The European Society of Cardiology and The North American Society of Pacing and Electrophysiology (1996). Heart rate variability - standards of measurement, physiological interpretation, and clinical use. *European Heart Journal*, *17*(3), 354–381.

Thanou, A., Stavrakis, S., Dyer, J., Munroe, M. E., James, J. A., & Merrill, J. T. (2016). Impact of heart rate variability, a marker for cardiac health, on lupus disease activity. *Arthritis Research & Therapy*, *18*.

Thayer, J. F., Åhs, F., Fredrikson, M., Sollers, J. J., & Wager, T. D. (2012). A meta-analysis of heart rate variability and neuroimaging studies: Implications for heart rate variability as a marker of stress and health. *Neuroscience & Biobehavioral Reviews*, *36*(2), 747–756.

Trites, R. (2023). Grooved pegboard test.

Wang, Q. (2012). Kernel principal component analysis and its applications in face recognition and active shape models. arXiv abs/1207.3538.

Wang, R., & Bi, H.-Y. (2022). A predictive model for chinese children with developmental dyslexia—Based on a genetic algorithm optimized back-propagation neural network. *Expert Systems with Applications*, *187*, Article 115949.

Wang, T., Chen, X., Zhang, X., Zhou, S., Feng, Q., & Huang, M. (2023). Multi-view imputation and cross-attention network based on incomplete longitudinal and multimodal data for conversion prediction of mild cognitive impairment. *Expert Systems with Applications*, Article 120761.

Wang, S., Fashanu, O. E., Zhao, D., Guallar, E., Gottesman, R. F., Schneider, A. L., et al. (2019). Relation of elevated resting heart rate in mid-life to cognitive decline over 20 years (from the Atherosclerosis Risk in Communities [ARIC] study). *The American Journal of Cardiology*, *123*(2), 334–340.

Weinstein, G., Davis-Plourde, K., Beiser, A. S., & Seshadri, S. (2021). Autonomic imbalance and risk of dementia and stroke: The framingham study. *Stroke*, *52*(6), 2068–2076.

Xiao, R., Xu, Y., Pelter, M., Fidler, R., Badilini, F., Mortara, D., et al. (2018). Monitoring significant ST changes through deep learning. *Journal of Electrocardiology*, *51*, S78–S82.

Yamakawa, T., Miyajima, M., Fujiwara, K., Kano, M., Suzuki, Y., Watanabe, Y., et al. (2020a). Wearable epileptic seizure prediction system with machine-learning-based anomaly detection of heart rate variability. *Sensors*, *20*(14).

Yamakawa, T., Miyajima, M., Fujiwara, K., Kano, M., Suzuki, Y., Watanabe, Y., et al. (2020b). Wearable epileptic seizure prediction system with machine-learning-based anomaly detection of heart rate variability. *Sensors (Basel, Switzerland)*, *20*.

Yang, A. C., Tsai, S.-J., Hong, C.-J., Yang, C.-H., Hsieh, C.-H., & Liu, M.-E. (2008). Association between heart rate variability and cognitive function in elderly community-dwelling men without dementia: A preliminary report. *Journal of the American Geriatrics Society*, *56*, 958–960.

Zubrikhina, M., Abramova, O., Yarkin, V., Ushakov, V., Ochneva, A., Bernstein, A., et al. (2023). Machine learning approaches to mild cognitive impairment detection based on structural MRI data and morphometric features. *Cognitive Systems Research*, *78*, 87–95.